Effect of the miR-26a/b-5p-STAT3-YKL-40 regulatory axis on proliferation, migration, and invasion of endometrial cancer cells

XINZHAO SUN*, SHANSHAN LIN*, XUEYAN ZHONG*, YANLU LUO, JIAHUANG YANG and JIANGTAO FAN

Department of Gynecology, The First Affiliated Hospital of Guangxi Medical University, Nanning, Guangxi 530021, P.R. China

Received September 30, 2025; Accepted April 6, 2026

DOI: 10.3892/or.2026.9132

Abstract. The incidence of endometrial cancer (EC) is on the rise annually, emphasizing the importance of timely diagnosis and treatment. Signal transducer and activator of transcription 3 (STAT3) has been identified as a proto-oncogene involved in multiple signaling pathways affecting various biological processes, especially in tumours. The aim of the present study was to validate the impact of STAT3 on EC phenotype and investigate its upstream and downstream regulatory mechanisms. Immunohistochemical analysis was conducted to assess STAT3 expression in EC tissues, followed by dual luciferase assays to confirm the regulatory relationship between STAT3 and microRNA (miR)-26a/b-5p. The effects of STAT3 and miR-26a/b-5p on HEC-1A cell proliferation and metastasis were evaluated through Cell Counting Kit-8 assays, cell scratch assays, and Transwell assays. Co-immunoprecipitation assays verified the binding between STAT3 and chitinase-3-like protein 1 (CHI3L1, also known as YKL-40). The results demonstrated high STAT3 expression in EC, associated with disease progression. miR-26a/b-5p directly targeted STAT3. Upregulated STAT3 enhanced HEC-1A cell proliferation, migration, and invasion, counteracting the inhibitory effects of miR-26a/b-5p on cell migration and invasion. In addition, it was confirmed that STAT3 binds to and promotes the expression of YKL-40. These findings contribute to clarifying the pathogenesis of EC.

Correspondence to: Dr Jiangtao Fan, Department of Gynecology, The First Affiliated Hospital of Guangxi Medical University, 6 Shuangyong Road, Nanning, Guangxi 530021, P.R. China
E-mail: jt_fan2018@163.com

*Contributed equally

Abbreviations: CHI3L1 and YKL-40, chitinase-3-like protein 1; EC, endometrial cancer; JAK, Janus kinase; STAT3, signal transducer and activator of transcription 3; TILs, tumor-infiltrating lymphocytes; VEGF, vascular endothelial growth factor

Key words: endometrial cancer, STAT3, microRNA-26a-5p, microRNA-26b-5p, chitinase-3-like protein 1

Introduction

Endometrial cancer (EC) is a gynecological cancer characterized by a rapidly increasing global incidence and associated mortality rate. According to statistics, there were over 420,000 new cases of corpus uteri cancer worldwide in 2022 (1). While EC predominantly affects postmenopausal women, there is a rising incidence among younger women. Early detection and diagnosis of EC at the low-grade stage have been revealed to be associated with a favorable prognosis, whereas diagnosis at the advanced stages has been associated with a reduced chance of survival (2,3).

The STAT3 protein with 770 amino acids regulates cell survival, differentiation, and proliferation. Notably, STAT3 has been shown to contribute to the development of cancers, such as myeloma, as well as breast and lung cancers due to its inherent ability to enhance proliferation and metastasis of tumor cells, as well as induce chemo-resistance and immune suppression. In human cancers, over-activation of STAT3 has been demonstrated to be associated with dismal outcomes (4-6). Specifically, STAT3 has been shown to regulate invasion, proliferation, drug resistance, and angiogenesis of EC cells. Research has established that angiogenesis is a crucial process in the development of tumors. Vascular cancer-associated fibroblasts, which are components of the tumor microenvironment, facilitate angiogenesis by promoting the expression of vascular endothelial cadherin and Vimentin, as well as the epithelial-to-endothelial transition through the IL-10/JAK1/STAT3 pathway. These events have been established to induce angiogenesis, thereby promoting EC progression (7). Research indicates that lncRNA NEAT1 binds to microRNA (miRNA or miR)-361, resulting in the upregulation of STAT3, which regulates the levels of factors including myeloid cell leukemia 1, Survivin, and vascular endothelial growth factor (VEGF)-A, thereby promoting the proliferation of EC cells and their resistance to chemotherapy. Furthermore, activation of STAT3 was identified as a critical factor that enhances invasiveness and stem cell-like properties of EC cells (8). Other factors that have been shown to significantly contribute to the progression of EC are obesity-related signals, such as estrogen and leptin, which facilitate the interaction between the estradiol-responsive gene leukemia inhibitory factor and the JAK family of cytoplasmic tyrosine kinases, including tyrosine kinase 2. This interaction results in the activation of STAT3, thereby amplifying the signaling pathways. The enhanced STAT3 activity contributes to the pro-invasive

activation of stromal fibroblasts, which enhances EC progression (9). The levels and activation of STAT3 are modulated by various signals and cytokines, and miRNA has been reported as a key regulator of STAT3 and its signaling pathways (10).

miRNAs are highly conserved non-coding RNA molecules, which modulate the transcription of genes by binding to the 3 'UTR of target mRNAs, leading to their inhibition or silencing (11). With the increasing in-depth research, several miRNAs have been identified to be either tumor suppressors or oncogenes, playing vital roles in nearly all key cellular processes (12). For instance, miR-26a/b-5p are potential tumor-suppressive microRNAs that exhibit decreased expression levels in a majority of solid tumors. They function as tumor suppressors by targeting multiple oncogenes, thereby inhibiting the malignant behavior of various tumor cell types. For example, miR-26a/b-5p has been shown to exert significant inhibitory effects on bladder cancer cells (13,14). Additionally, miR-26a/b-5p has been demonstrated to modulate STAT3 pathway activity, with bioinformatics analyses indicating a potential reciprocal relationship between them; however, the roles of both miR-26a/b-5p and STAT3 pathway, as well as their regulatory relationships in EC remains incompletely understood, thereby requiring further investigations.

Chitinase-3-like protein 1 (CHI3L1, also known as YKL-40) was identified as a downstream target of STAT3 (15). It was shown to be regulated by STAT3 in astrocytes and glioma cells and to stimulate cell invasion and migration (16). YKL-40, a glycoprotein encoded by the CHI3L1 gene and secreted by cells such as macrophages, chondrocytes, neutrophils, and cancer cells, is enriched in various cancer types and implicated in their progression (17-19). The signaling mechanisms of YKL-40 were shown to modulate proliferation, infiltration, apoptosis, CD4 T-cell Th2 polarization, and angiogenesis (20). A previous study revealed that siRNA targeting YKL-40 silences its expression, thereby inhibiting the metastasis and proliferation of EC cells (21). However, the association between STAT3 and YKL-40 in EC is poorly understood.

In the present study, the role and mechanisms of STAT3 in EC progression were investigated to provide a basis for the development of novel STAT3-targeted interventions for EC treatment.

Materials and methods

Cell culture. HEC-1A cell line (cat. no. CL-0099), 293T cell line (cat. no. CL-0005), and McCoy's 5A medium (cat. no. PM150710) were purchased from Wuhan Punosai Life Science and Technology Co., Ltd. Fetal bovine serum (FBS) was procured from Dalian Meilun Biotechnology Co., Ltd. McCoy's 5A Medium and DMEM High Glucose Medium (Gibco; Thermo Fisher Scientific, Inc.), both containing 10% FBS, were used to culture HEC-1A cells and 293T cells, respectively. Cryopreserved cells were removed from the -80˚C freezer, rapidly thawed, and then cultured in a 37˚C incubator with regular cell passaging.

Tissue sample collection. The study was approved (approval no. 2024-E211-01) by the Ethics Committee of the First Affiliated Hospital of Guangxi Medical University (Nanning, China). Both EC tissues and corresponding paracancerous endometrial tissues from a total of 45 patients diagnosed with primary EC were retrospectively collected. The age of the patients ranged from 31 to 78 years. These patients had undergone initial surgical treatment at our hospital between January 2021 and February 2022. The tissue samples were preserved by the Department of Pathology at our hospital. The inclusion criteria were as follows: i) No prior treatment related to the disease; ii) absence of concomitant malignant tumors; and iii) absence of severe systemic diseases. Paracancerous endothelial tissues were excised at a distance of 2 cm or more from the cancerous tissues. The present study was conducted in accordance with the guidelines of the Declaration of Helsinki and the ethics committee of the hospital. Additionally, all study participants provided their written informed consent prior to recruitment.

Immunohistochemical (IHC) staining. Tissues were fixed in 4% paraformaldehyde at 4˚C for 24 h. After fixation, tissue samples were prepared into pathological sections through paraffin embedding and slicing. The sections were cut at a thickness of 4 μm. The slides were baked at 60˚C for 2 h. Deparaffinization and rehydration were performed using xylene and a graded ethanol series. Antigen retrieval was carried out under high pressure using citrate buffer (cat. no. MVS-0066; Fuzhou Maixin Biotech Co., Ltd.). Subsequently, an SP kit (cat. no. SP-0022, BIOSS) was used according to the manufacturer's instructions: Endogenous peroxidase activity was blocked using the 3% hydrogen peroxide solution provided in the SP kit. After washing, the sections were incubated with the normal goat serum blocking solution from the same kit at room temperature for 15-20 min. The sections were sequentially incubated with a specific STAT3 antibody (1:200; cat. no. bs-1141R; BIOSS) at 4˚C overnight, followed by incubation with biotinylated secondary antibody working solution (ready-to-use; from the SP-0022 kit) at room temperature for 15-20 min, and then with horseradish peroxidase-conjugated streptavidin working solution (ready-to-use; from the SP-0022 kit) at room temperature for 15-20 min. The sections were then stained with 3,3'-diaminobenzidine (DAB; cat. no. ZLI-9018, ZSGB-BIO) at room temperature for 2 min, counterstained with hematoxylin (cat. no. S0142; BIOSS) at room temperature for 1 min, differentiated in hydrochloric alcohol, dehydrated, and finally mounted with neutral balsam. Images of five random fields (magnification, x200) were captured under an inverted optical microscope. The staining results were quantitatively analyzed using ImageJ software (version 1.51j8; National Institutes of Health). Grayscale signal values were converted into optical density (OD) values. The integrated OD (IOD) divided by the area of target protein distribution (IOD/Area) yielded the average OD (AOD).

Lentiviral transduction. Lentiviruses for STAT3 overexpression were purchased from Sangon (Shanghai) Biotech Co., Ltd. Lentiviruses for miR-26a/b-5p overexpression, YKL-40 overexpression, and STAT3 knockdown were obtained from GeneChem Co., Ltd. The lentiviruses used in the present study were purchased as ready-to-use preparations. The shRNA sequence for STAT3 knockdown was designed based on a validated Qiagen sequence: sh-STAT3: 5'-CAGCCTCTCTGC AGAATTCAA-3'. The negative control sh-NC was designed

Table I. Primer sequences.

Gene	Sequence
miR-26a-5p	F: 5'-ACCAAGTAATCCAGGATAGGCTAAA-3'
miR-26b-5p	F: 5'-ATCGGGTAATTCAGGATAGGTAAAA-3'
U6	F: 5'-GGAACGATACAGAGAAGATTAGC-3'
	R: 5'-TTGAACGCTTCACGAATTTGCG-3'
STAT3	F: 5'-ACAGGTTGGACATGATGCACAC-3'
	R: 5'-TAAGCCTTTGCCCTGCATGA-3'
YKL-40	F: 5'-TGTTCCGAGGTCAGGAGGAT-3'
	R: 5'-TGCCCATCACCAGCTTACTG-3'
GAPDH	F: 5'-GCACCGTCAAGGCTGAGAAC-3'
	R: 5'-TGGTGAAGACGCCAGTGGA-3'

miR, microRNA; STAT3, signal transducer and activator of transcription 3; YKL-40, chitinase-3-like protein 1.

using the sequence of Qiagen AllStars Negative Control: 5'-CAGGGTATCGACGATTACAAA-3' (22). Lentiviral transduction was performed according to the manufacturer's instructions. The multiplicity of infection (MOI) used was 20, and HitransG A (GeneChem Co., Ltd.) was added to enhance transduction efficiency according to the manufacturer's protocol. HEC-1A cells were seeded into 24-well plates, and transduction was carried out the following day when the cell confluence reached ~30%. Subsequently, 16 h after transduction, the transduction medium was replaced with complete culture medium for further incubation. At 48 h post-transduction, antibiotic selection was initiated using complete culture medium containing either 600 μg/ml geneticin (G418) (cat. no. MA0321; Dalian Meilun Biotechnology Co., Ltd.) for miR-26a/b-5p and YKL-40 overexpression constructs or 2.5 μg/ml puromycin (cat. no. P8230; Solarbio Life Sciences) for STAT3 overexpression and knockdown constructs.

Reverse transcription-quantitative PCR (RT-qPCR). Total miRNA or mRNA was extracted from HEC-1A cells in healthy growth conditions using RNAiso Plus (cat. no. 9108, Takara Bio, Inc.). RNA was separated by adding chloroform, precipitated by adding isopropanol, washed with 75% ethanol, and finally dissolved in an appropriate volume of RNase-free water. miRNA was reverse transcribed using a tailing method (Mir-X™ miRNA First Strand Synthesis Kit; cat. no. 638315; Takara Bio, Inc.). The resulting cDNA was diluted 10-fold with RNase-free water and used for subsequent PCR amplification. For mRNA, genomic DNA removal and reverse transcription were performed using the PrimeScript™ RT Reagent Kit (cat. no. RR047; Takara Bio, Inc.). All cDNA amplifications were performed using TB Green Premix Ex Taq II (cat. no. RR820A; Takara Bio, Inc.) on an ABI 7500 Fast qPCR system under the following reaction conditions: Pre-denaturation at 95˚C for 30 sec (1 cycle); denaturation at 95˚C for 5 sec, annealing and extension at 60˚C for 34 sec (40 cycles). The relative expression levels of target genes were calculated using the $2^{-\Delta\Delta Cq}$ method (23). The primer sequences are listed in Table I. The U6 primer was designed and synthesized by Sangon Biotech (Shanghai) Co., Ltd. The primers for GAPDH, miR-26a-5p, miR-26b-5p, STAT3, and YKL-40 were designed and synthesized by Takara Biotechnology (Beijing) Co., Ltd.

Cell proliferation assay. Briefly, 5,000 HEC-1A cells per well were inoculated into a 96-well plate, with the experiments conducted in triplicate or more for each group. A blank control group was established. Cell Counting Kit-8 (CCK-8) reagent (cat. no. MA0218-10; Dalian Meilun Biotechnology Co., Ltd.) was added at 0, 24, 48, 72, and 96 h after inoculation and the wells were incubated at 37˚C for 1 h (24). The OD was recorded at 450 nm using an enzyme-labeler and the cell proliferation curve was generated using the measurements.

Cell scratch assay. The prepared cell suspension was incubated in a 6-well plate with a concentration of $2.5x10^6$ HEC-1A cells per well. Before inoculation, the bottom surface of the plate was marked with horizontal lines. Cells were serum-starved for 8 h prior to scratching. When the cell confluence reached over 90%, a scratch was created using a 200-μl pipette tip. Subsequently, the scraped cells were aspirated and 2 ml of serum-free medium was added. Images of the cells were captured immediately and at 24-h intervals using an inverted light microscope (Leica Microsystems GmbH), with the wound healing rate at 48 h calculated (25). Wound healing was quantified by measuring the wound area using ImageJ software (version 1.51j8). The wound closure ratio was calculated as (area at 0 h-area at 48 h)/area at 0 h.

Transwell migration and invasion assays. In the migration assay, 600 μl of McCoy's 5A medium supplemented with 20% FBS was added to each well of a 24-well plate. A small chamber with an 8-μm pore size (Corning, Inc.) containing $5x10^4$ cells in 100 μl of serum-free McCoy's 5A medium was placed into each well. The cells were incubated at 37˚C for 48 h in a CO_2 incubator. After 48 h, the non-migrated cells on the upper surface of the membrane were discarded and those that migrated were fixed using 4% paraformaldehyde (cat. no. P1110; Solarbio Life Sciences) at room temperature for 15 min and stained using 0.1% crystal violet at room temperature for 10 min. The cells were then observed and counted

using an inverted light microscope equipped with a 10X objective lens. A total of five random fields per well were counted. The invasion assay followed a similar procedure, except for the addition of diluted Matrigel (cat. no. 356234; Corning, Inc.) before the cells were seeded (25). Matrigel was diluted 1:16 in serum-free McCoy's 5A medium, and 100 μl of the diluted Matrigel was added to the upper chamber and incubated at 37˚C overnight. The Matrigel simulated the extracellular matrix, allowing for the evaluation of the invasive potential of the cells. ImageJ software (version 1.51j8) was used for analysis.

Western blotting (WB). RIPA lysis buffer (cat. no. PC101; EpiZyme) was used to lyse the HEC-1A cells. Protein concentration was determined using a BCA kit. The cell lysate was collected and mixed with loading buffer (cat. no. 1610747; Bio-Rad Laboratories, Inc.), followed by incubation at 100˚C for 10 min. Equal amounts of protein (50 μg per lane) were loaded onto a 10% SDS-PAGE gel. SDS-PAGE was performed at 150 V for 60 min, and the proteins were then transferred onto a PVDF membrane at 200 mA for 1 h (26). The membrane was blocked with a protein-free rapid blocking buffer (cat. no. PS108; EpiZyme) at room temperature for 15 min, followed by incubation with primary antibodies at 4˚C overnight. The primary antibodies used were: STAT3 (1:3,000; cat. no. 9139S; Cell Signaling Technology, Inc.), YKL-40 (1:1,000; cat. no. PA5-43746; Invitrogen; Thermo Fisher Scientific, Inc.), β-tubulin (1:10,000; cat. no. 66240-1-Ig; Proteintech Group, Inc.), β-actin (1:10,000; cat. no. MA5-15739; Invitrogen; Thermo Fisher Scientific, Inc.), and GAPDH (1:5,000; cat. no. 60004-1-Ig; Proteintech Group, Inc.). Subsequently, the membranes were incubated with corresponding species-specific fluorescent goat anti-rabbit IgG (H+L) secondary antibodies, DyLight™ 800 4X PEG (1:10,000; cat. no. SA5-35571, Invitrogen; Thermo Fisher Scientific, Inc.) in the dark at room temperature for 45 min. Finally, PVDF membranes were scanned using an Odyssey infrared imaging system. ImageJ software (version 1.51j8) was used to analyze the band intensity of the collected band images, and normalization was performed based on the ratio of the target protein to the internal reference protein.

Dual luciferase activity assay. The potential binding sites between miR-26a-5p/26b-5p and the STAT3 3'-UTR were predicted using RNAhybrid (http://bibiserv.cebitec.uni-bielefeld.de/rnahybrid). The 3'-untranslated region (3'-UTR) of STAT3 containing the miR-26a/b-5p binding site was synthesized and inserted into the pmirGLO luciferase vector by Genepharma Co., Ltd. to construct wild-type (STAT3-WT) and mutant-type (STAT3-MUT) STAT3 reporter plasmids [cat. no. C09005; Genomeditech (Shanghai) Co., Ltd.] Corresponding mimics (miR-26a-5p, miR-26b-5p, and miR-NC: 5'-UUCUCCGAACGUGUCACGUTT-3') were also synthesized (cat. no. B02001; Genepharma Co., Ltd.) 293T cells were prepared as single-cell suspensions and seeded into 12-well plates at a density of $5x10^5$ cells per well, followed by incubation for 24 h. A mixture of reporter vector and mimics was pre-prepared. Subsequently, Lipofectamine 2000 transfection reagent (cat. no. G04004; Genepharma Co., Ltd.), pre-diluted in serum-free medium, was added and mixed gently, and the transfections complexes were allowed to stand for 20 min. The transfection complexes were then added to the cells cultured in 12-well plates and incubated for 6 h. After 6 h, the transfection mediume was replaced with complete culture medium, and the cells were further cultured for 48 h. Cells were processed using a dual luciferase reporter assay kit (cat. no. G06001; GenePharma Co., Ltd.). First, PLB lysis buffer (part of the luciferase assay kit) was added, and the resulting cell lysate was transferred into wells of a microplate reader plate. Subsequently, Firefly and *Renilla* luciferase reaction reagents were added sequentially. Luminescence values were measured using a BioTek multimode microplate reader (Agilent Technologies, Inc.) equipped with Gen5 software. Finally, Firefly luciferase activity was normalized to *Renilla* luciferase activity (Firefly/*Renilla* ratio). The aforementioned steps were performed in accordance with the manufacturer's instructions.

Co-immunoprecipitation (Co-IP). Total protein was extracted through lysis of HEC-1A cells using NP-40 cell lysis buffer (cat. no. P0013F; Beyotime Institute of Biotechnology). The lysate was centrifuged at 12,000 x g for 12 min at 4˚C to remove debris. A total of 35 μl of Protein A/G Magnetic Beads (cat. no. HY-K0202; MedChemExpress) were collected into EP tubes and washed twice with PBST, then mixed with STAT3 antibody (12 μg; from a 30-μg/ml stock; cat. no. 9139S; Cell Signaling Technology, Inc.) or IgG antibody (12 μg; from a 30-μg/ml stock; mouse; cat. no. B900620; Proteintech Group, Inc.) in a total volume of 400 μl. The mixture was incubated at 25˚C with gentle rotation for 30 min to allow antibody-bead coupling. The beads were retained and washed with PBST to remove unbound antibodies, and then 400 μl of the extracted total protein was added and mixed by rotation at 4˚C for 2 h. The beads were then retained and unbound protein was thoroughly washed. Finally, the magnetic beads were eluted to obtain protein samples and subjected to western blot analysis using the primary antibodies at the following concentrations: STAT3 (Cell Signaling Technology, Inc.) and YKL-40 (1:1,000; rabbit; cat. no. 12036-1-AP; Proteintech Group, Inc.) (27).

Protein docking analysis. The proteins were first prepared using Discovery Studio software 4.5 (https://www.3ds.com/products/biovia/discovery-studio). The processed protein structures were then visualized using PyMOL 2.5 (https://pymol.org). The 3D structures of STAT3 and YKL-40 were obtained from UniProt (https://www.uniprot.org) and subsequently imported into Discovery Studio for protein-protein docking analysis, which was performed using the ZDOCK module.

Bioinformatics analysis. The expression levels of YKL-40 in EC tumor samples and non-tumor samples were analyzed using the GEPIA2 database (http://gepia2.cancer-pku.cn/). Protein-protein interactions between STAT3 and CHI3L1 were predicted using the STRING database (https://string-db.org/).

Statistical analysis. Results are presented as the mean ± standard deviation (SD). Statistical analyses were performed using SPSS 23.0 software (IBM Corp.). Data with a normal distribution were compared using unpaired Student's t-test, whereas one-way ANOVA was used to compare

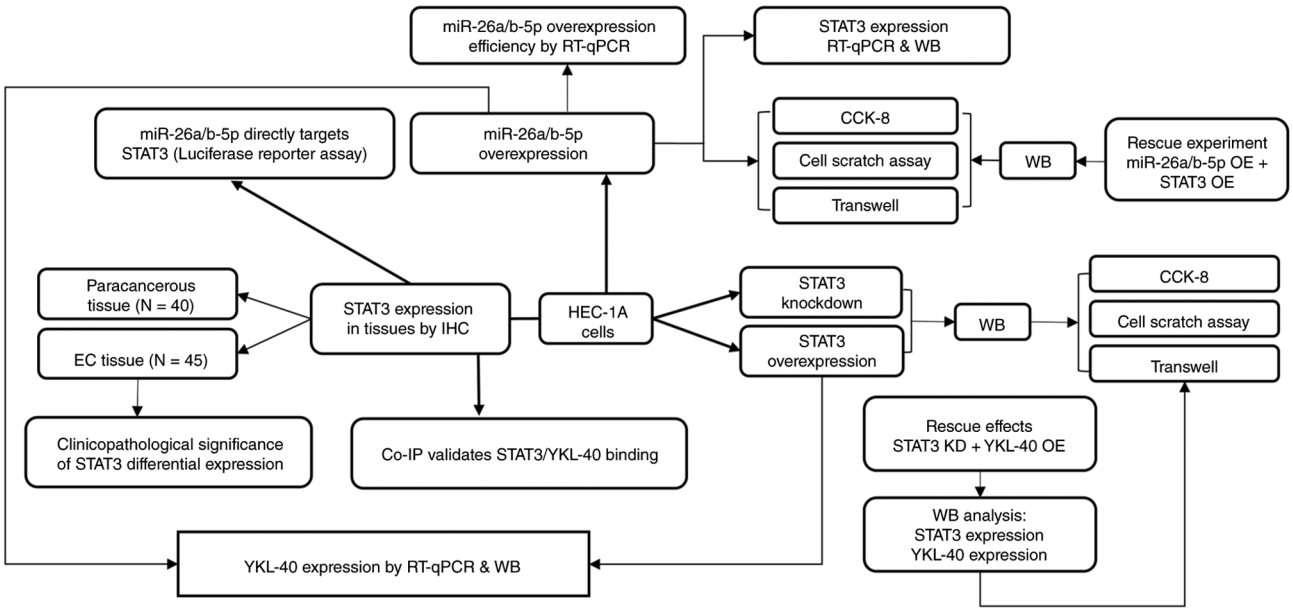

Figure 1. Technical roadmap of the study. miR, microRNA; RT-qPCR, reverse transcription-quantitative PCR; STAT3, signal transducer and activator of transcription 3; WB, western blotting; OE, overexpression; EC, endometrial cancer; IHC, immunohistochemistry; Co-IP, co-immunoprecipitation; YKL-40, chitinase-3-like protein 1; KD, knockdown.

three or more groups, followed by Tukey's HSD post hoc test (equal variances) or Tamhane's T2 test (unequal variances). Non-normally distributed data were analyzed using Mann-Whitney U test (for two groups) or Kruskal-Wallis H test with Dunn's post hoc test (for three or more groups). All experiments were conducted in triplicate. Notably, $P<0.05$ was considered to indicate a statistically significant difference. All the diagrams were drawn using Adobe Illustrator and GraphPad Prism 10 (Dotmatics).

Results

Experimental workflow. The overall experimental design and workflow are shown in Fig. 1.

STAT3 is predominantly expressed and at higher levels in EC tissues. The protein STAT3 has been identified as a proto-oncogene (28), and to elucidate its role in EC, IHC staining for STAT3 was performed on EC tissues collected from 45 patients and on paracancerous tissues from 40 patients, as shown in Fig. 2A. All representative images are shown in the Fig. S1. Notably, five paracancerous tissue samples were not included in the analysis because they were located less than 2 cm from the cancerous tissues. Before analysis, statistical tests were conducted to confirm that there was no difference in age among patients from the cancerous and paracancerous tissue groups. The staining results were quantified and statistically analyzed. As shown in Fig. 2B, STAT3 expression levels were significantly higher in EC tissues than in adjacent normal tissues. Various clinicopathological parameters of these 45 patients were collected and statistically analyzed, with the analysis indicating that the STAT3 level was higher in cancer tissues characterized by lower differentiation rates and aggressive infiltration of the muscularis propria; additionally, a high level of STAT3 was associated with the formation of pulvinar cancer thrombus in patients (Table II). Notably, STAT3 was upregulated in EC and was associated with malignant progression of EC. While evaluating STAT3 expression in tumor cells, it was noticed that the expression of total STAT3 in tumor-infiltrating lymphocytes (TILs) was heterogeneous; that is, scattered STAT3-positive lymphocytes were observed in a few samples, whereas most samples showed negative TILs, which may be related to the immunosuppressive tumor microenvironment (29).

STAT3 promotes the progression of HEC-1A cells in vitro. HEC-1A cell models overexpressing and silencing STAT3 were constructed, and the levels of STAT3 after silencing or overexpression were confirmed using WB (Fig. 3A and B). The CCK-8 proliferation and scratch assays demonstrated that overexpression of STAT3 promoted proliferation and healing of HEC-1A cells (Fig. 3C and E), whereas silencing of STAT3 achieved the opposite results (Fig. 3D and F). Transwell experiments showed that overexpressed STAT3 levels markedly enhanced cell migration and invasion (Fig. 3G and H), whereas its downregulation decreased the number of migrated and invasive cells (Fig. 3I and J). Therefore, it was concluded that STAT3 promotes EC cell progression *in vitro*.

miR-26a/b-5p targets STAT3 and downregulates its expression. Research has identified miRNAs as factors of interest in tumor suppression (30). The predicted binding sites between STAT3 and miR-26a/b-5p are shown in Fig. 4A. Subsequently, dual luciferase tests were performed to verify these interactions. miR-26a/b-5p mimics and STAT3-WT or STAT3-MUT vectors were transfected into 293T cells. Notably, the incorporation of miR-26a/b-5p suppressed firefly luciferase activity following STAT3-WT vector transfection (Fig. 4B). Moreover, STAT3 mRNA and protein expression

Table II. Clinical and pathological significance of STAT3.

Clinical parameter	N	Mean rank	Z	P-value
Differentiation				
G_1	23	18.89	-2.147	0.032[a]
G_{2-3}	22	27.30		
Myometrial invasion				
≤1/2	32	20.23	-2.217	0.027[a]
>1/2	13	29.81		
Vascular cancer embolus				
No	33	20.47	-2.144	0.032[a]
Yes	12	29.96		
Diameter of tumor (cm)				
≤3.5	27	23.72	-0.452	0.651
>3.5	18	21.92		
FIGO staging				
I-II	35	23.54	-0.519	0.604
III	10	21.10		
Lymphatic metastasis				
No	39	23.40	-0.518	0.605
Yes	6	20.42		
Adnexal invasion				
No	40	22.71	-0.416	0.678
Yes	5	25.30		

[a]P<0.05. STAT3, signal transducer and activator of transcription 3.

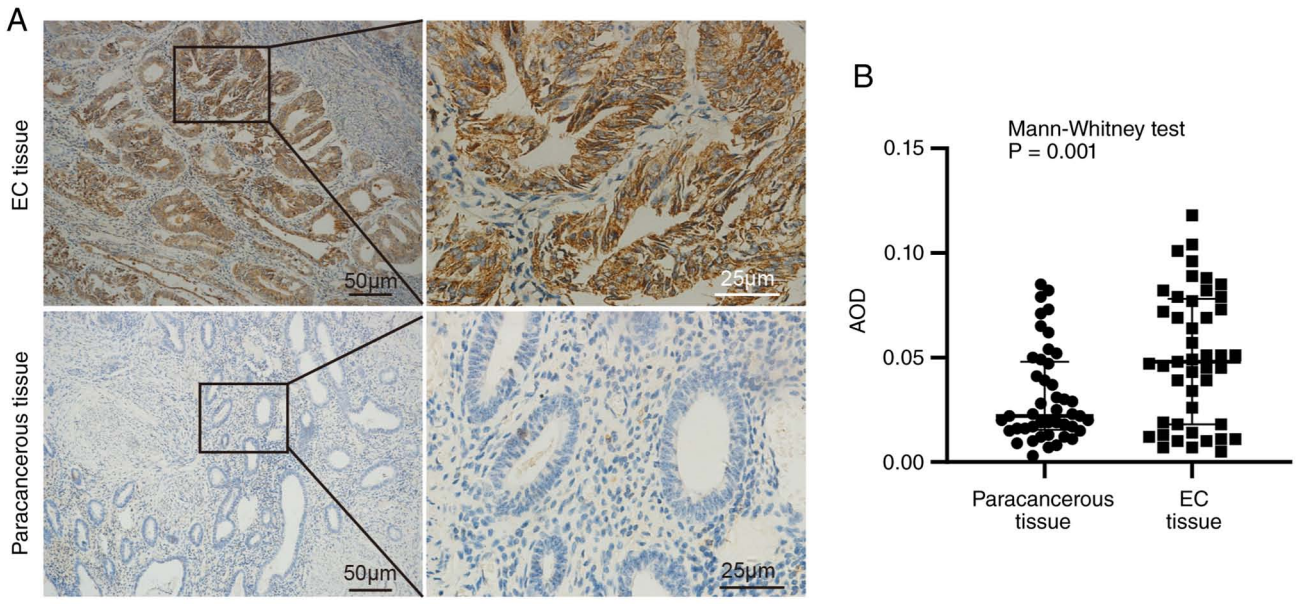

Figure 2. Expression of STAT3 in EC tissues. (A) The STAT3 expression profile in EC tissues (n=45) and paracancerous endometrial tissues (n=40) was detected using IHC staining. (B) Quantitative analysis of STAT3 expression in EC tissues (n=45) and para-carcinoma intima tissues (n=40). STAT3, signal transducer and activator of transcription 3; EC, endometrial cancer; AOD, average optical density.

were decreased following miR-26a/b-5p overexpression (Fig. 4C and D). These findings suggest that miR-26a/b-5p targeting of STAT3 suppresses STAT3 transcription.

miR-26a/b-5p suppresses the migration and invasion of HEC-1A cells in vitro. The enrichment of miR-26a/b-5p was promoted in HEC-1A cells to assess their effects on the

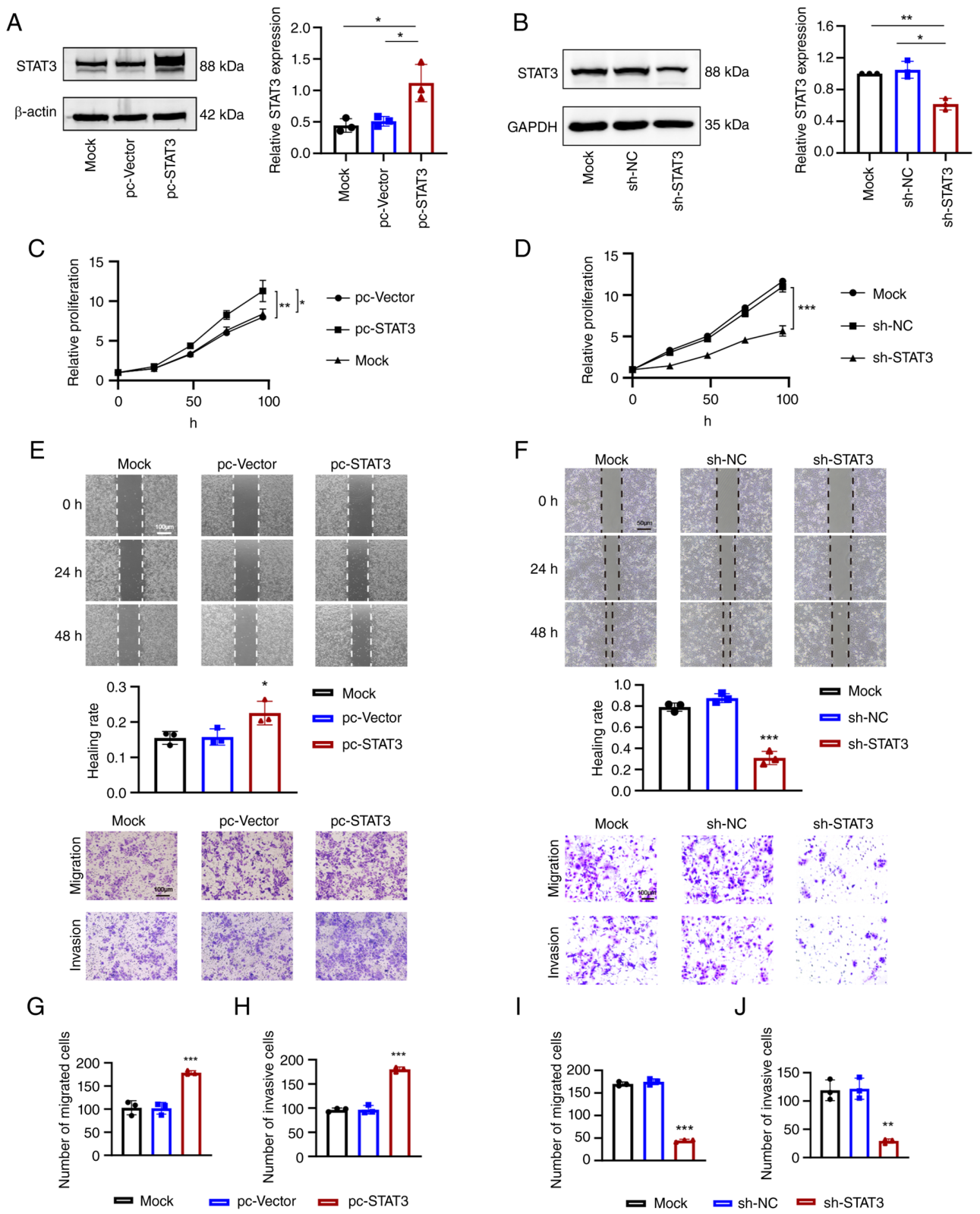

Figure 3. STAT3 promotes proliferation and migration of HEC-1A cells. (A and B) Western blotting verified the overexpression and silencing efficacy of STAT3. (C and D) Cell Counting Kit-8 assay revealed that overexpression of STAT3 promoted cell proliferation, whereas knockdown of STAT3 had the opposite effect. (E and F) Overexpression of STAT3 promoted cell wound healing, whereas knockdown of STAT3 had the opposite effect. (G-J) Transwell assay showed that overexpression of STAT3 promoted cell migration and invasion, while knockdown exerted the opposite effect. *P<0.05, **P<0.01 and ***P<0.001. STAT3, signal transducer and activator of transcription 3; sh-, short hairpin; NC, negative control.

cellular characteristics of these cells. Transduction efficiency was quantified using RT-qPCR, and the results revealed that miR-26a/b-5p was successfully enriched in HEC-1A cells, with more than a 20-fold increase in its expression levels (Fig. 5A). Cell scratch, CCK-8 cell proliferation, and Transwell assays were conducted. While no significant effect on cell

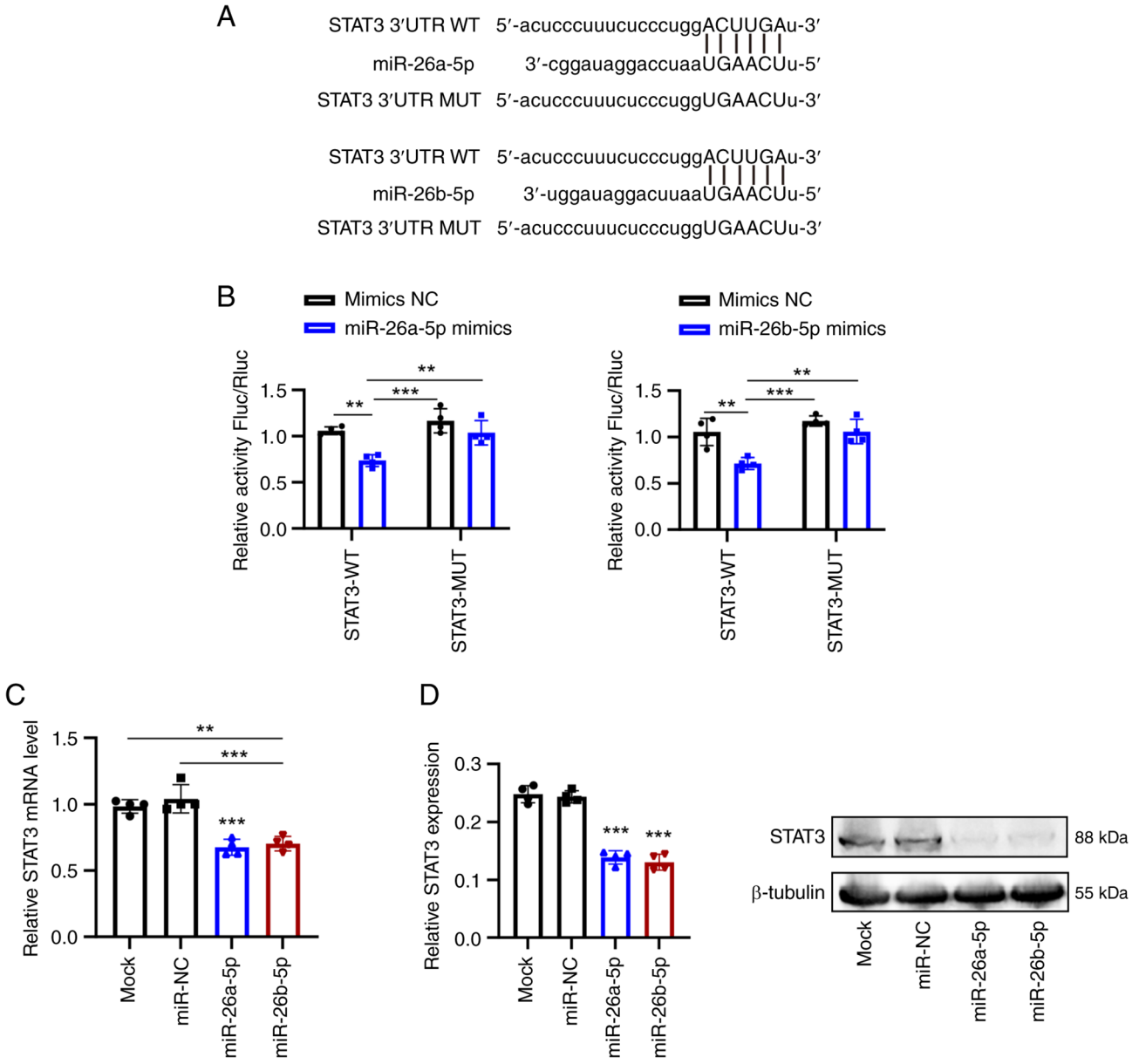

Figure. 4. miR-26a/b-5p targets STAT3. (A) STAT3 wild-type vector and mutant vector sequences. (B) Dual luciferase activity assay. (C and D) Overexpression of miR-26a/b-5p reduces the mRNA and protein levels of STAT3 in cells. **P<0.01 and ***P<0.001. miR, microRNA; STAT3, signal transducer and activator of transcription 3; WT, wild-type; MUT, mutant; NC, negative control; Fluc, firefly luciferase; Rluc, *Renilla* luciferase.

proliferation was observed (Fig. 5B), miR-26a/b-5p markedly inhibited the wound healing of HEC-1A cells (Fig. 5C). Concurrently, the number of migrated and invasive cells was markedly reduced (Fig. 5D and E). These observations indicated that miR-26a/b-5p inhibits the migratory and invasive behavior of EC cells *in vitro*.

Upregulation of STAT3 primarily abrogates the inhibitory effects of miR-26a/b-5p on HEC-1A cell migration and invasion. The association between miR-26a/b-5p and STAT3 suggested that miR-26a/b-5p may influence cellular behavior by regulating the expression of STAT3. To verify this, changes in the biological properties of cells were observed by overexpressing STAT3 in the miR-26a/b-5p-treated cell group. It was found that STAT3 was successfully enriched in miR-26a-5p + pc-STAT3 and miR-26b-5p + pc-STAT3 group cells, as detected using WB (Fig. 6A). CCK-8 assays showed that both miR-26a-5p and miR-26b-5p significantly suppressed cell proliferation compared with wild-type cells (P<0.05, Fig. 6B and C). STAT3 reversed the anti-proliferative effect of miR-26b-5p (Fig. 6C). However, STAT3 did not significantly reverse the effect of miR-26a-5p (Fig. 6B). By contrast, cell scratch and Transwell assays revealed that the introduction of STAT3 strongly abolished the inhibitory effects of miR-26a/b-5p on cell healing, migration, and invasion (Fig. 6D-F). These results suggest that STAT3 is a critical component in the regulatory pathway of miR-26a/b-5p.

STAT3 binds to YKL-40 and activates YKL-40 gene transcription. As a potential diagnostic marker for EC, YKL-40 was analyzed through the GEPIA2 database, and the results revealed higher levels of YKL-40 in EC tumor samples compared with

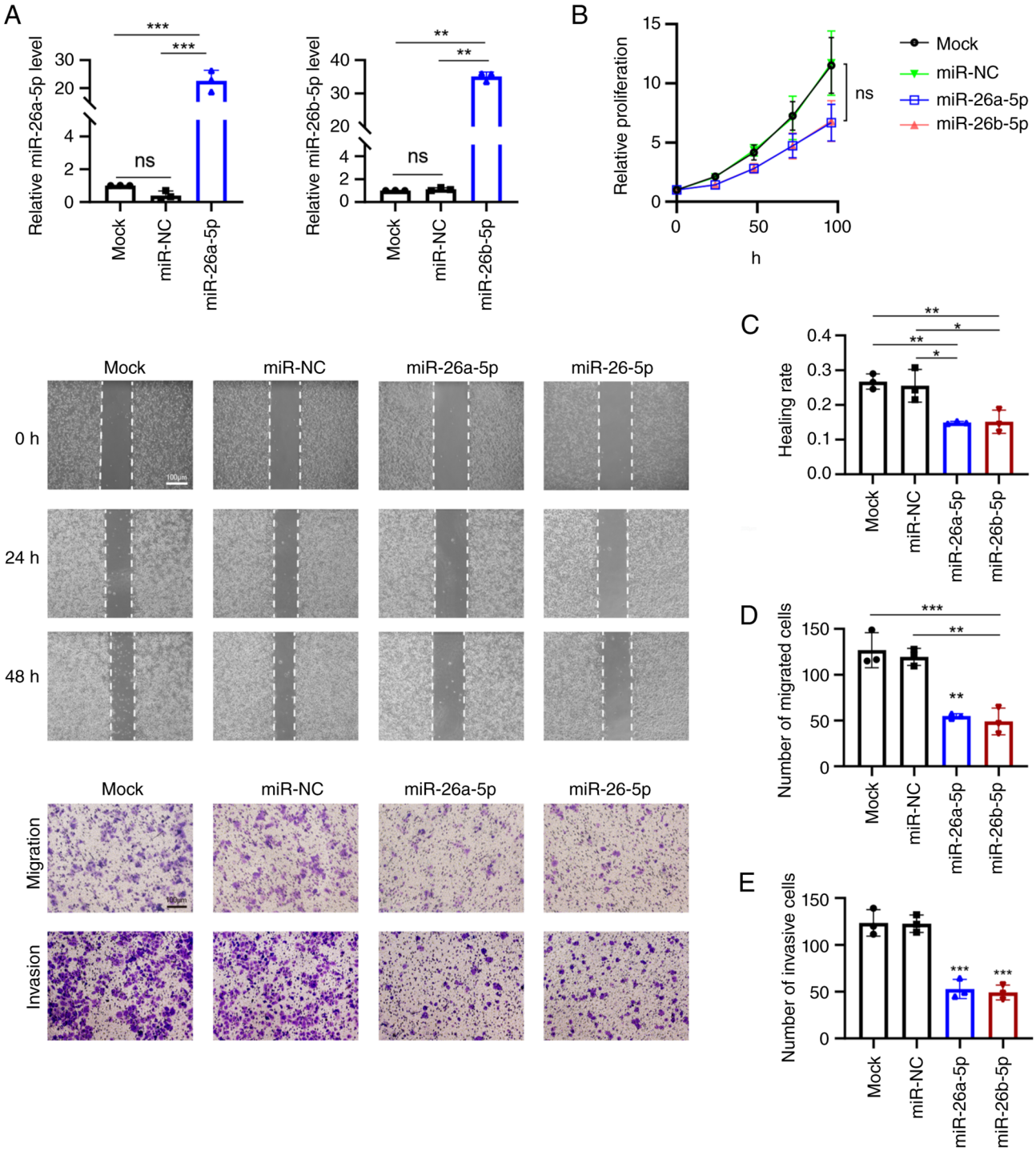

Figure 5. miR-26a/b-5p reduces the migration and invasion activity of HEC-1A cells. (A) miR-26a/b-5p Transduction efficiency was measured, indicating successful overexpression of miR-26a/b-5p. (B) Cell Counting Kit-8 cell proliferation assay, (C) wound healing assay, and (D and E) Transwell migration and invasion assays were used to evaluate the effects of miR-26a/b-5p on cell proliferation, migration, and invasion. *P<0.05, **P<0.01 and ***P<0.001. miR, microRNA; STAT3, signal transducer and activator of transcription 3; NC, negative control; ns, not significant.

those in non-tumor samples (Fig. 7A). It was revealed in our previous study that preoperative serum YKL-40 levels were elevated in patients with EC relative to patients with leiomyoma and healthy women (31). To verify whether STAT3 regulates YKL-40 expression in EC, further analysis was conducted. As shown in Fig. 7B, the STRING database analysis suggested a potential interaction between STAT3 and CHI3L1, supported by multiple lines of evidence. To further investigate this interaction at the structural level, protein-protein docking analysis was performed, and the predicted binding mode is shown in Fig. 7C. Subsequently, Co-IP experiments using a STAT3 antibody to precipitate STAT3 from total proteins suggested that YKL-40 protein was detected in the immunoprecipated complex, indicating an interaction between YKL-40 and STAT3 (Fig. 7D). Further analysis revealed that mRNA and protein expression of YKL-40 was promoted in HEC-1A cells overexpressing STAT3 (Fig. 7E and F). By contrast, overexpression of miR-26a/b-5p resulted in a decrease of YKL-40

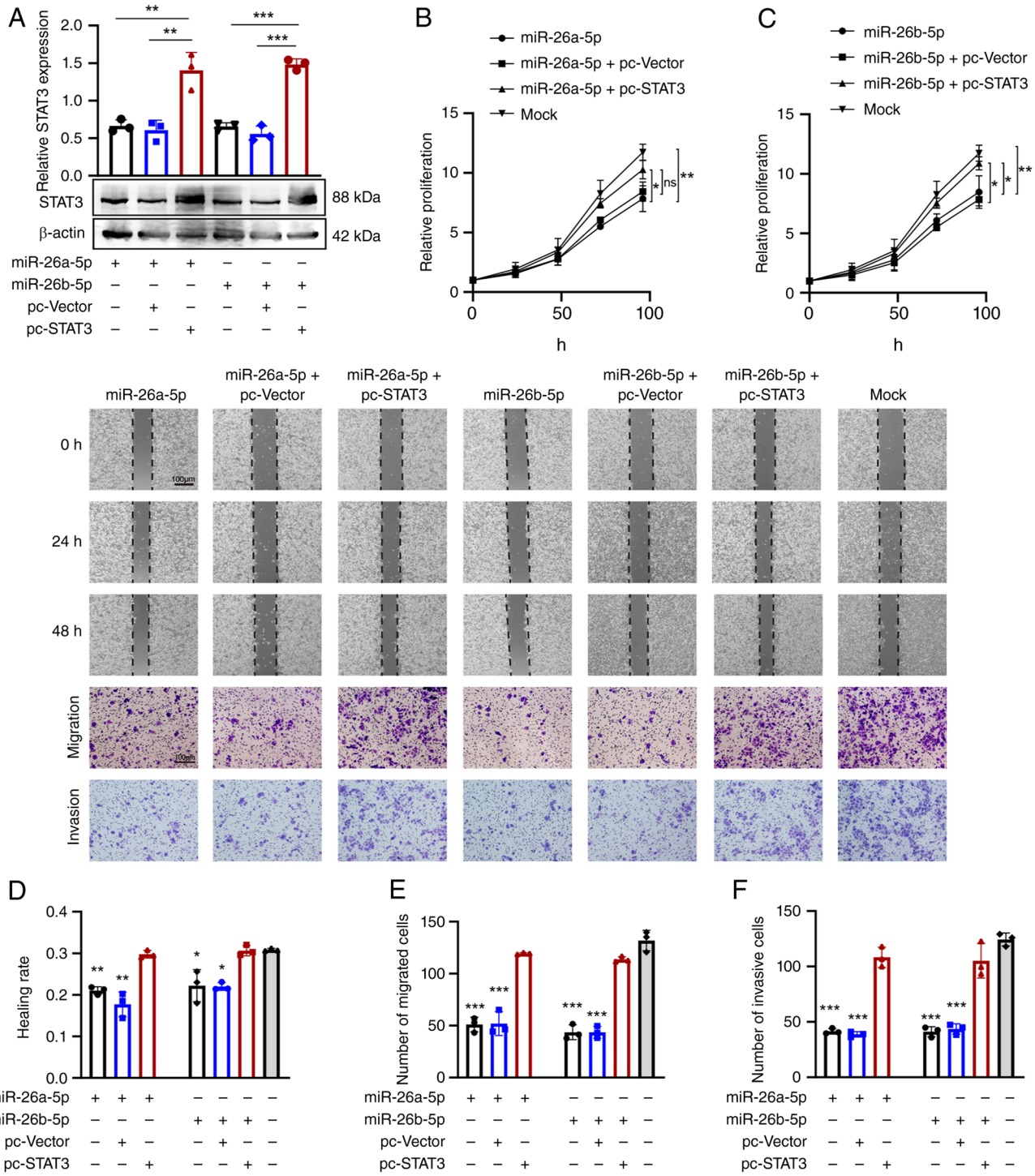

Figure 6. Overexpression of STAT3 counteracts the suppressive effect of miR-26a/b-5p on the cellular biological behavior. (A) STAT3 was reintroduced into cells overexpressing miR-26a/b-5p, and STAT3 protein expression in each group was detected by western blotting. (B and C) Cell Counting Kit-8 assay, (D) wound healing assay, and (E and F) Transwell migration and invasion assays were used to determine whether STAT3 overexpression reversed the inhibitory effects of miR-26a/b-5p on cell proliferation, migration, and invasion. *P<0.05, **P<0.01 and ***P<0.001. STAT3, signal transducer and activator of transcription 3; miR, microRNA; ns, not significant.

mRNA and protein levels (Fig. 7G and H). These findings indicated that STAT3 binds to YKL-40 protein in EC cells and promotes YKL-40 expression, whereas miR-26a/b-5p, a negative regulator of STAT3, inhibits YKL-40 expression.

STAT3 promotion of cell proliferation and migration is dependent on YKL-40. To verify whether the pro-carcinogenic effect of STAT3 was dependent on YKL-40, YKL-40 was upregulated in the sh-STAT3 group of cells. Prior to this, it was validated that YKL-40 could be successfully upregulated by overexpression in wild-type HEC-1A cells, as confirmed by WB (Fig. S2). Subsequently, the changes in the levels of YKL-40 and STAT3 proteins in each group were verified using WB (Fig. 8A and B). It was found that upregulated

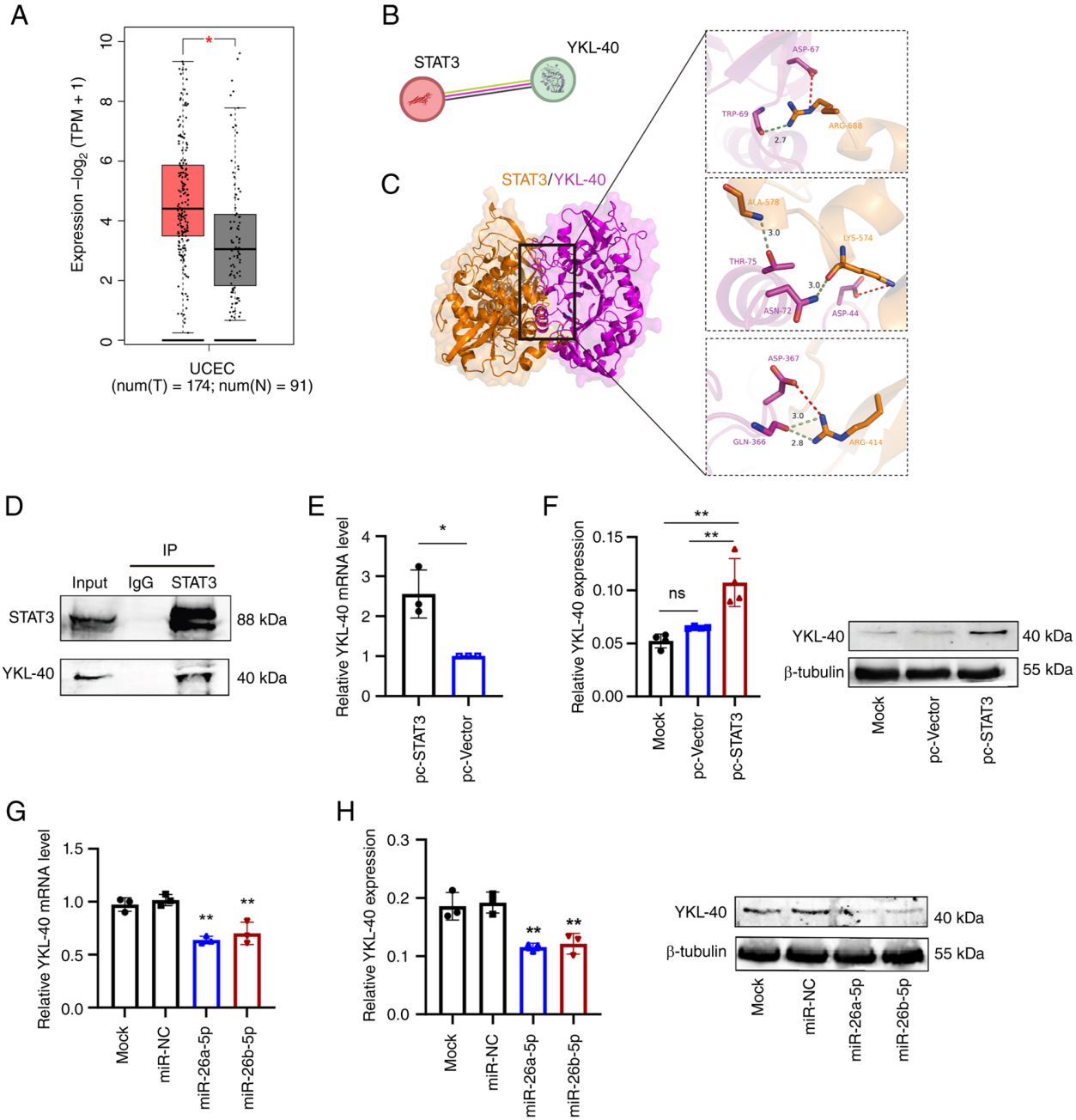

Figure 7. STAT3 modulates YKL-40 expression. (A) Expression analysis of YKL-40 in tumor and non-tumor samples from the GEPIA2 database. (B) STRING database analysis of the protein-protein interaction between STAT3 and CHI3L1 (the gene encoding YKL-40). Purple lines indicate experimentally determined interactions, green lines represent text-mining evidence, and gray lines denote co-expression evidence. (C) Three-dimensional interaction between YKL-40 and STAT3. (D) Co-immunoprecipitation assay showing the interaction of STAT3 and YKL-40. (E and F) STAT3 overexpression induced YKL-40 levels. (G and H) Overexpression of miR-26a/b-5p led to downregulation of YKL-40 mRNA and protein expression levels. *P<0.05 and **P<0.01. STAT3, signal transducer and activator of transcription 3; CHI3L1 and YKL-40, chitinase-3-like protein 1; IP, immunoprecipitation; NC, negative control; miR, microRNA.

YKL-40 did not promote STAT3 protein expression. By contrast, STAT3 knockdown was observed to decrease the migratory potential, invasiveness, proliferation, and wound healing abilities of the cells. Based on these observations, YKL-40 levels were upregulated in the cells, and all these abilities were restored (Fig. 8C-F). These findings suggest that the pro-carcinogenic impact of STAT3 is significantly mediated via YKL-40.

The role of the miR-26a/b-5p-STAT3-YKL-40 axis in EC progression was investigated. As shown in the diagram of Fig. 9, downregulation of miR-26a/b-5p led to STAT3 activation, which in turn promoted malignant progression through its interaction with YKL-40.

Discussion

In the present study, through the integration of clinical tissue sample analysis, *in vitro* cellular functional experiments, and molecular mechanism validation, the regulatory role of the miR-26a/b-5p-STAT3-YKL-40 signaling axis in

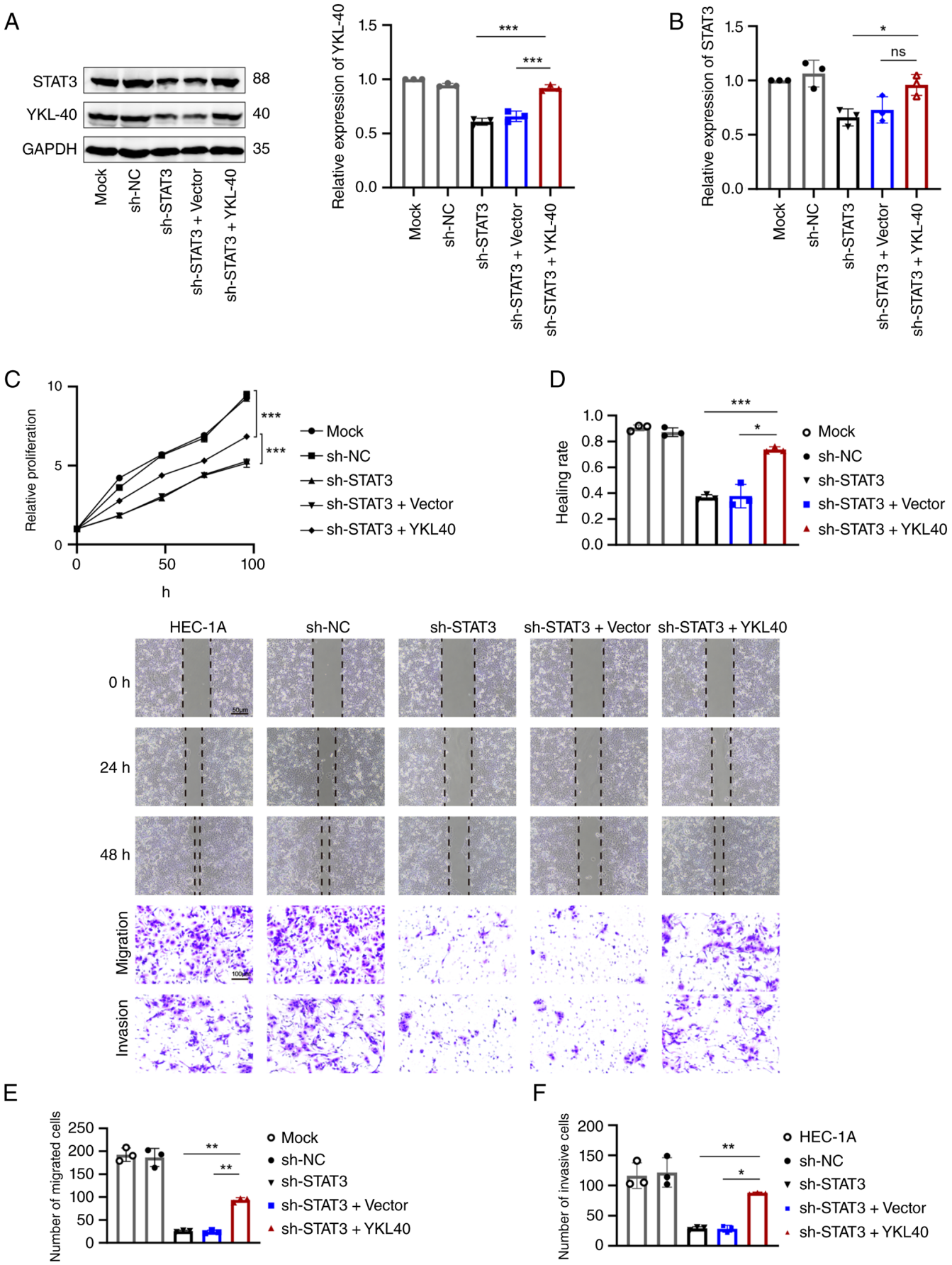

Figure 8. Pro-carcinogenic effect of STAT3 is dependent on YKL-40. (A and B) The expression levels of YKL-40 and STAT3 in each group of cells was quantified using western blotting. Results of the (C) Cell Counting Kit-8 assay, (D) cell scratch assay, and (E and F) Transwell migration and invasion assays. *P<0.05, **P<0.01 and ***P<0.001. STAT3, signal transducer and activator of transcription 3; YKL-40, chitinase-3-like protein 1; sh, short hairpin; NC, negative control; ns, not significant.

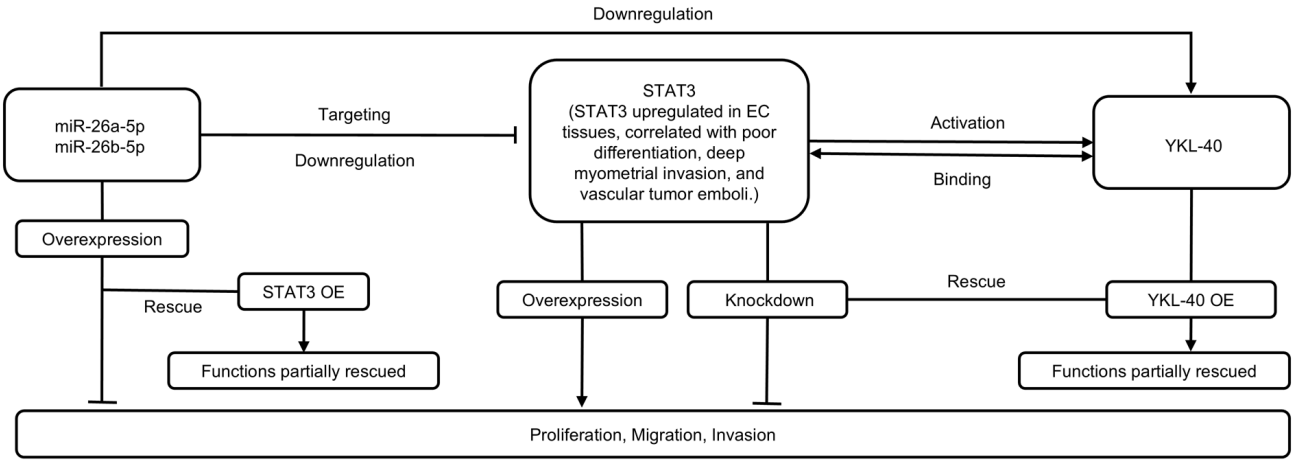

Figure 9. Schematic diagram of the proposed mechanism of STAT3 in endometrial cancer. miR, microRNA; STAT3, signal transducer and activator of transcription 3; EC, endometrial cancer; YKL-40, chitinase-3-like protein 1; OE, overexpression.

the progression of endometrial cancer was systematically elucidated. Statistical analysis not only confirmed the central driving role of STAT3 in EC but also revealed a clear causal chain between the loss of upstream regulation and the activation of downstream effects, providing a novel perspective for understanding the molecular pathogenesis of EC.

Immunohistochemical analysis of EC tissue samples in the present study revealed that STAT3 expression levels were significantly higher in tumor tissues than in adjacent normal tissues, and its high expression was significantly positively associated with several key clinicopathological parameters indicative of tumor progression ($P<0.05$). Specifically, STAT3 expression levels showed an increasing trend with decreasing tumor differentiation grade (from Grade I to Grade III), deeper myometrial invasion, and the presence of cancer thrombus formation. These findings are consistent with research that considers STAT3 a marker of poor prognosis in various malignant tumors (10). *In vitro* functional experiments further supported this conclusion mechanistically: HEC-1A cells overexpressing STAT3 exhibited enhanced growth and metastatic capabilities, whereas STAT3 knockdown produced the opposite effects. These clinical and *in vitro* findings mutually corroborate each other, collectively establishing the important role of STAT3 in the malignant progression of EC.

To elucidate the underlying molecular mechanisms that could regulate STAT3, miRNAs were focused on. The cell cycle regulation of endometrial cells by miRNAs is important for tumorigenesis due to the cyclic changes of endometrial cells that lead to frequent proliferation and shedding (32). miRNA profiling analysis of EC showed reduced expression of 14 miRNAs with tumor suppressive effects, including miR-26b-5p and miR-26a-5p (33). Based on bioinformatics predictions and dual-luciferase reporter gene experiments, it was confirmed that miR-26a-5p and miR-26b-5p can directly target the 3'-UTR region of STAT3. Functionally, overexpression of miR-26a/b-5p can significantly downregulate STAT3 protein expression and effectively inhibit the migration, and invasion abilities of EC cells. However, no significant inhibitory effect on cell proliferation was observed. This discrepancy may be attributed to differences in the sensitivity of migration/invasion vs. proliferation to regulation by miR-26a-5p and miR-26b-5p, or to the specific experimental conditions employed in this study. Moreover, the anti-proliferative effects of these miRNAs may require additional factors or distinct cellular environments to manifest. Further studies are therefore needed to elucidate their precise role in EC cell proliferation. Nevertheless, restoring STAT3 expression can partially reverse the tumor-suppressive effects caused by miR-26a/b-5p. The role of miR-26a/b-5p as upstream inhibitory factors of STAT3 in EC is clarified by these results, and it is suggested that their downregulation or loss may be one of the important reasons for abnormal activation of STAT3 in EC.

Further research found that STAT3 can mediate the aforementioned pro-cancer effects by regulating its downstream target gene YKL-40. As a transcriptional target of STAT3, YKL-40 has been confirmed to promote tumor angiogenesis and enhance the migration and invasion abilities of tumor cells (34,35). YKL-40 has also been reported to be highly expressed in patients with EC and closely associated with poor prognosis (36). The present study found that the expression level of STAT3 was positively associated with the expression of YKL-40. Rescue experiments further confirmed that the inhibitory effect of STAT3 knockdown on EC cell activity could be partially reversed by exogenous YKL-40, indicating that STAT3 mediates its pro-tumor effects at least in part through YKL-40. In addition, it was observed for the first time that STAT3 protein directly binds to YKL-40 protein in EC cells. According to a recent study, Yu *et al* (27) confirmed that in glioblastoma, CHI3L1 enhances the transcriptional activity of STAT3 by directly binding to its coiled-coil domain, thereby promoting malignant tumor progression. This provides an important mutual verification with the present study, revealing the protein interaction of STAT3-YKL-40 in different tumor types, suggesting that this may represent a conserved oncogenic mechanism in various cancers and providing a theoretical basis for the subsequent development of broad-spectrum antitumor strategies.

These research findings suggest that, given the central driving role of STAT3 in EC, the targeting of STAT3 or its upstream and downstream regulatory factors is expected to become an effective strategy for inhibiting tumor progression. For example, BBI608, a STAT3 inhibitor, was effective

in reducing the cell viability of *in vitro*-specific primary progenitor cells in patients with EC at a specific concentration and its efficacy could be enhanced by combining it with paclitaxel (37). Additionally, research has shown that the application of ruxolitinib and nifuroxazide, small molecule inhibitors of JAK1 and STAT3, inhibited IL6/JAK1/STAT3 signaling. This inhibition significantly reduced the growth of tumor cells and reduced the activity of cancer stem cells in EC both *in vitro* and *in vivo* (38). Additionally, delivering miR-26a/b-5p into EC cells may exert antitumor effects. As demonstrated in a related study, loading miR-326 onto nanoparticles and transfecting it into cancer stem cells in EC tissues could downregulate the expression levels of STAT3/VEGF, and thereby inhibit cancer stem cell activity (39). YKL-40, as a terminal effector molecule of this axis, represents an attractive therapeutic target. Nevertheless, translating this fundamental discovery into clinical practice still faces numerous challenges, including how to achieve efficient targeted delivery, how to avoid off-target effects, and how to screen potential beneficiaries, all of which need to be further explored and validated through subsequent in-depth research.

However, the present study also has certain limitations. First, all gain- and loss-of-function experiments were conducted solely in the HEC-1A cell line, which may not fully represent the role of this signaling axis in EC. Second, all current experiments are limited to *in vitro* settings. Although they reveal direct regulatory relationships between molecules, they cannot fully recapitulate the authentic tumor growth and metastatic processes *in vivo*. Whether miR-26a/b-5p mimics or STAT3 inhibitors can effectively suppress tumor growth *in vivo*, as well as the therapeutic efficacy and safety of targeting this signaling axis, still require further validation through the establishment of EC xenograft models. Furthermore, the clinical tissue samples in this study lack subsequent follow-up data, precluding further analysis of the association between this signaling axis and patient survival outcomes. In view of this, our subsequent research will focus on validating the core findings in additional EC cell lines and establishing subcutaneous or orthotopic tumor models in nude mice to evaluate the *in vivo* antitumor effects of intervening in this signaling axis. Concurrently, follow-up data will be collected to analyze its prognostic value. These efforts will provide more robust preclinical evidence for future clinical translation.

In conclusion, it was shown that STAT3 is highly expressed in EC tissues and promotes EC progression. Additionally, STAT3 was demonstrated to upregulate its binding protein, YKL-40. miR-26a/b-5p was shown to act as a tumor-suppressive factor in EC, inhibiting cancer cell metastasis and proliferation through direct targeting of STAT3.

Acknowledgements

Not applicable.

Funding

The present study was financed by both the National Natural Science Foundation of China (grant no. 81960464) and the Guangxi Science and Technology Planning Project (grant no. GuikeAB22080045).

Availability of data and materials

The data generated in the present study may be requested from the corresponding author.

Authors' contributions

XS, XZ and SL conducted the experiments and analyzed the data. XS and YL curated the data, conducted statistical analysis, and contributed to manuscript drafting. JY collected data and performed data analysis. JF provided financial support, contributed to experimental design, and revised the manuscript. XS and JF confirm the authenticity of all raw data. All authors reviewed and approved the final manuscript.

Ethics approval and consent to participate

The present study strictly complied with the privacy rights of human subjects. Written informed consent was obtained from all study participants. The present study was approved (approval no. 2024-E211-01) by the Ethics Committee of the First Affiliated Hospital of Guangxi Medical University (Nanning, China).

Patient consent for publication

Not applicable.

Competing interests

The authors declare that they have no competing interests.

References

1. Bray F, Laversanne M, Sung H, Ferlay J, Siegel RL, Soerjomataram I and Jemal A: Global cancer statistics 2022: GLOBOCAN estimates of incidence and mortality worldwide for 36 cancers in 185 countries. CA Cancer J Clin 74: 229-263, 2024.
2. Makker V, MacKay H, Ray-Coquard I, Levine DA, Westin SN, Aoki D and Oaknin A: Endometrial cancer. Nat Rev Dis Primers 7: 88, 2021.
3. Liu J, Zhu W, Xia L, Zhu Q, Mao Y, Shen Y, Li M, Zhang Z and Du J: Identification of CAPG as a potential prognostic biomarker associated with immune cell infiltration and ferroptosis in uterine corpus endometrial carcinoma. Front Endocrinol (Lausanne) 15: 1452219, 2024.
4. Zou S, Tong Q, Liu B, Huang W, Tian Y and Fu X: Targeting STAT3 in cancer immunotherapy. Mol Cancer 19: 145, 2020.
5. Ma JH, Qin L and Li X: Role of STAT3 signaling pathway in breast cancer. Cell Commun Signal 18: 33, 2020.
6. Liu Y, Liao S, Bennett S, Tang H, Song D, Wood D, Zhan X and Xu J: STAT3 and its targeting inhibitors in osteosarcoma. Cell Prolif 54: e12974, 2021.
7. Yu Z, Zhang Q, Wei S, Zhang Y, Zhou T, Zhang Q, Shi R, Zinovkin D, Pranjol ZI, Zhang J and Wang H: CD146^{+}CAFs promote progression of endometrial cancer by inducing angiogenesis and vasculogenic mimicry via IL-10/JAK1/STAT3 pathway. Cell Commun Signal 22: 170, 2024.
8. Dong P, Xiong Y, Yue J, Xu D, Ihira K, Konno Y, Kobayashi N, Todo Y and Watari H: Long noncoding RNA NEAT1 drives aggressive endometrial cancer progression via miR-361-regulated networks involving STAT3 and tumor microenvironment-related genes. J Exp Clin Cancer Res 38: 295, 2019.
9. Viswanadhapalli S, Dileep KV, Zhang KYJ, Nair HB and Vadlamudi RK: Targeting LIF/LIFR signaling in cancer. Genes Dis 9: 973-980, 2021.
10. Galoczova M, Coates P and Vojtesek B: STAT3, stem cells, cancer stem cells and p63. Cell Mol Biol Lett 23: 12, 2018.

11. Pan C, Stevic I, Müller V, Ni Q, Oliveira-Ferrer L, Pantel K and Schwarzenbach H: Exosomal microRNAs as tumor markers in epithelial ovarian cancer. Mol Oncol 12: 1935-1948, 2018.
12. Fabris L, Ceder Y, Chinnaiyan AM, Jenster GW, Sorensen KD, Tomlins S, Visakorpi T and Calin GA: The potential of MicroRNAs as prostate cancer biomarkers. Eur Urol 70: 312-322, 2016.
13. Wu K, Mu XY, Jiang JT, Tan MY, Wang RJ, Zhou WJ, Wang X, He YY, Li MQ and Liu ZH: miRNA-26a-5p and miR-26b-5p inhibit the proliferation of bladder cancer cells by regulating PDCD10. Oncol Rep 40: 3523-3532, 2018.
14. Miyamoto K, Seki N, Matsushita R, Yonemori M, Yoshino H, Nakagawa M and Enokida H: Tumour-suppressive miRNA-26a-5p and miR-26b-5p inhibit cell aggressiveness by regulating PLOD2 in bladder cancer. Br J Cancer 115: 354-363, 2016.
15. Yan C, Ding X, Wu L, Yu M, Qu P and Du H: Stat3 downstream gene product chitinase 3-like 1 is a potential biomarker of inflammation-induced lung cancer in multiple mouse lung tumor models and humans. PLoS One 8: e61984, 2013.
16. Singh SK, Bhardwaj R, Wilczynska KM, Dumur CI and Kordula T: A complex of nuclear factor I-X3 and STAT3 regulates astrocyte and glioma migration through the secreted glycoprotein YKL-40. J Biol Chem 286: 39893-39903, 2011.
17. Wang Z, Wang S, Jia Z, Hu Y, Cao D, Yang M, Liu L, Gao L, Qiu S, Yan W, *et al*: YKL-40 derived from infiltrating macrophages cooperates with GDF15 to establish an immune suppressive microenvironment in gallbladder cancer. Cancer Lett 563: 216184, 2023.
18. Hao H, Chen H, Xie L and Liu H: YKL-40 promotes invasion and metastasis of bladder cancer by regulating epithelial mesenchymal transition. Ann Med 53: 1170-1178, 2021.
19. Böckelmann LC, Felix T, Calabrò S and Schumacher U: YKL-40 protein expression in human tumor samples and human tumor cell line xenografts: Implications for its use in tumor models. Cell Oncol (Dordr) 44: 1183-1195, 2021.
20. Zhao T, Su Z, Li Y, Zhang X and You Q: Chitinase-3 like-protein-1 function and its role in diseases. Signal Transduct Target Ther 5: 201, 2020.
21. Li L, Fan J, Li D, Liu Y, Shrestha P, Zhong C, Xia X and Huang X: Influence of YKL-40 gene RNA interference on the biological behaviors of endometrial cancer HEC-1A cells. Oncol Lett 16: 1777-1784, 2018.
22. Spitzner M, Roesler B, Bielfeld C, Emons G, Gaedcke J, Wolff HA, Rave-Fränk M, Kramer F, Beissbarth T, Kitz J, *et al*: STAT3 inhibition sensitizes colorectal cancer to chemoradiotherapy in vitro and in vivo. Int J Cancer 134: 997-1007, 2014.
23. Livak KJ and Schmittgen TD: Analysis of relative gene expression data using real-time quantitative PCR and the 2(-Delta Delta C(T)) method. Methods 25: 402-408, 2001.
24. Zhou X, Nie M, Xin X, Hua T, Zhang J, Shi R, Dong K, Shu W, Yan B and Wang H: RAB17 promotes endometrial cancer progression by inhibiting TFRC-dependent ferroptosis. Cell Death Dis 15: 655, 2024.
25. Zhang X, Cui D, Sun W, Yang G, Wang W and Mi C: Regulation of the β-catenin/LEF-1 pathway by the siRNA knockdown of RUVBL1 expression inhibits breast cancer cell proliferation, migration and invasion. Oncol Rep 53: 22, 2025.
26. Kurien BT and Scofield RH: Western blotting. Methods 38: 283-293, 2006.
27. Yu W, Gui S, Peng L, Luo H, Xie J, Xiao J, Yilamu Y, Sun Y, Cai S, Cheng Z and Tao Z: STAT3-controlled CHI3L1/SPP1 positive feedback loop demonstrates the spatial heterogeneity and immune characteristics of glioblastoma. Dev Cell 60: 1751-1767.e9, 2025.
28. Levy DE and Inghirami G: STAT3: A multifaceted oncogene. Proc Natl Acad Sci USA 103: 10151-10152, 2006.
29. Karras JG, Wang Z, Huo L, Howard RG, Frank DA and Rothstein TL: Signal transducer and activator of transcription-3 (STAT3) is constitutively activated in normal, self-renewing B-1 cells but only inducibly expressed in conventional B lymphocytes. J Exp Med 185: 1035-1042, 1997.
30. Wu HH, Leng S, Sergi C and Leng R: How MicroRNAs command the battle against cancer. Int J Mol Sci 25: 5865, 2024.
31. Fan JT, Si XH, Liao Y and Shen P: The diagnostic and prognostic value of serum YKL-40 in endometrial cancer. Arch Gynecol Obstet 287: 111-115, 2013.
32. Banno K, Yanokura M, Kisu I, Yamagami W, Susumu N and Aoki D: MicroRNAs in endometrial cancer. Int J Clin Oncol 18: 186-192, 2013.
33. Jayaraman M, Radhakrishnan R, Mathews CA, Yan M, Husain S, Moxley KM, Song YS and Dhanasekaran DN: Identification of novel diagnostic and prognostic miRNA signatures in endometrial cancer. Genes Cancer 8: 566-576, 2017.
34. Dankner M, Maritan SM, Priego N, Kruck G, Nkili-Meyong A, Nadaf J, Zhuang R, Annis MG, Zuo D, Nowakowski A, *et al*: Invasive growth of brain metastases is linked to CHI3L1 release from pSTAT3-positive astrocytes. Neuro Oncol 26: 1052, 2024.
35. Pouyafar A, Heydarabad MZ, Mahboob S, Mokhtarzadeh A and Rahbarghazi R: Angiogenic potential of YKL-40 in the dynamics of tumor niche. Biomed Pharmacother 100: 478-485, 2018.
36. Kemik P, Saatli B, Yıldırım N, Kemik VD, Deveci B, Terek MC, Koçtürk S, Koyuncuoğlu M and Saygılı U: Diagnostic and prognostic values of preoperative serum levels of YKL-40, HE-4 and DKK-3 in endometrial cancer. Gynecol Oncol 140: 64-69, 2016.
37. Chen J, Huang S, Li H, Li Y, Zeng H, Hu J, Lin Y, Cai H, Deng P, Song T, *et al*: STAT3 inhibitor BBI608 reduces patient-specific primary cell viability of cervical and endometrial cancer at a clinical-relevant concentration. Clin Transl Oncol 25: 662-672, 2023.
38. van der Zee M, Sacchetti A, Cansoy M, Joosten R, Teeuwssen M, Heijmans-Antonissen C, Ewing-Graham PC, Burger CW, Blok LJ and Fodde R: IL6/JAK1/STAT3 signaling blockade in endometrial cancer affects the ALDHhi/CD126+ stem-like component and reduces tumor burden. Cancer Res 75: 3608-3622, 2015.
39. Gao Y, Qian H, Tang X, Du X, Wang G, Zhang H, Ye F and Liu T: Superparamagnetic iron oxide nanoparticle-mediated expression of miR-326 inhibits human endometrial carcinoma stem cell growth. Int J Nanomedicine 14: 2719-2731, 2019.